Materials Physics and Mechanics 27 (2016) 133-141 Received: July 9, 2016

TRANSPARENT FILMS FROM ALUMINIUM-DOPED ZINC OXIDE FIBERS PREPARED BY ELECTROSPINNING METHOD

V.I. Kondratiev[1*], I. Kink[1,2], A.E. Romanov[3], L. Dolgov[1]

[1]Institute of Physics, University of Tartu, W. Ostwaldi 1, Tartu, 50411, Estonia

[2]Kompest Ltd, Puiestee 13b, Tartu, 50303, Estonia

[3]ITMO University, Kronverskiy 49, St. Petersburg, 197101, Russian Federation

*e-mail: kondraty@ut.ee

Abstract. Aluminium doped zinc oxide films were prepared by electrospinning method through deposition of fibers from sol-gel solution on a substrate. Samples were specially annealed after deposition. Several annealing temperatures and heating and cooling rates are examined. Two preparation routes giving both thin fibers with diameter near 40 nm and thick fibers with diameter near 140 nm are elaborated. Samples were characterized by optical spectrophotometry, scanning electron microscopy and energy dispersive X-ray spectroscopy. Light transmittance of prepared films is 85-90 % in the visible spectral range. However transmittance of samples annealed in air is slightly higher than for samples annealed in vacuum. This slight decrease in transmittance can be associated with higher content of carbon in the samples annealed in vacuum.

1. Introduction

Transparent conductive films (TCF) are an important constructive part for such modern optoelectronic devices as solar cells, light-emitting diodes, electro-optical glasses. Nowadays, tin-doped indium oxide (ITO) is widely produced as transparent conductive oxide (TCO) standard for TCF applications. High price of indium [1] and limitation of world indium reserves [2] stipulated the search of alternative conductive oxides and improvement of their preparation procedures.

Doped zinc oxide, particularly aluminum doped zinc oxide (AZO), is one of the promising materials which potentially can replace ITO. Desirable parameters of TCF films are quite high, up to 85 %, transmittance, and at the same time low electrical resistivity in the range of 10^{-4} Ω-cm [3]. Thickening of film and increasing of the doping level enhance electrical conductivity, but decrease the optical transmittance of film. Therefore properties of certain AZO film in each case are a compromise between better optical or electrical behaviour. Different scientific groups try to achieve better parameters for AZO films developing such preparation techniques as molecular beam epitaxy [4], chemical vapor deposition [5], pulsed laser deposition [6], spray pyrolysis [7], spin-coating [8], electrospinning [9–11].

Here electrospinning technique is considered as a method allowing the covering of surface by the more or less dense network made of AZO fibers [9–13]. Proper amount of meshes in the network will allow to keep the necessary high level of optical transmittance. At the same time electrical conductivity could be provided by developed system of overlappings and intersections of fibers. In comparison with other methods electrospinning does not require complicated and expensive equipment. It's possible to control film dimensions and thickness

© 2016, Institute of Problems of Mechanical Engineering

via shape and size of electrospun nanofibers, and deposition time. Moreover, electrospinning of different solutions at the same time can help to produce films with desirable parameters [14].

There are some reports about application of electrospinned AZO films in photovoltaic devices [3, 10] and catalytic surfaces [9]. At the same time there are a set of questions, which are still require solutions. For example, it is needed to protect thin AZO fibers from the excessive granulation [15], coalescence [16] and cracking to keep the proper morphology of the AZO network. Here we propose the routes for preparation of AZO fibers both with smaller 40-100 nm and with bigger 100-150 nm diameters. Control of their granulation and coalescence states is realized by means of variation of annealing conditions, humidity and level of the Al doping. Eventually we worked out two preparation routes named as route #1 and route #2, which slightly differ by viscosity of precursors, applied voltages and feeding rates for fibers resulting in a different length of fibers and their distribution on the surface. We paid a special attention to the control of fibers' properties by changing atmosphere and temperature during their annealing. Concentration of Al dopant was varied by small steps in order to trace the changes in electrical properties of the samples.

2. Experimental procedure

2.1 Electrospinning procedure. The scheme of self-made electrospinning set-up is represented in Fig. 1. Potential of the power supply (h) (~ 25 kV) was applied to the two metal disks forming uniform electric field in the region of fiber formation. Sample was attached to the left metal disk (collector) (a) covered with aluminum foil. The piston of syringe (e) with polymer solution was pushed by pump (i) in order to form a droplet at the end of the needle. Electric field deformed a droplet into a Taylor cone [17]. When the surface tension forces become lower than electric forces the polymer jet arises from the Taylor cone. Such kind of jet comes to the collector and stick to it in form of fiber. So after some time of deposition a network from overlapped fibers forms the layer on the collector.

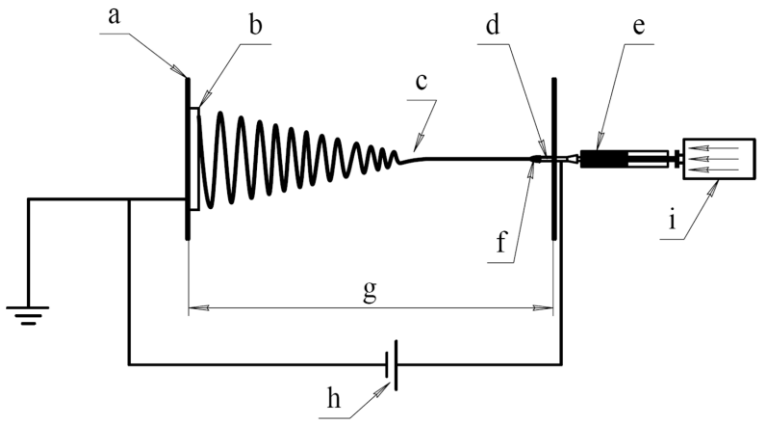

Fig. 1. Self-made electrospinning set-up: a) metal disk (collector) b) sample c) fiber jet d) needle e) syringe with solution f) Taylor cone g) distance h) voltage power supply i) syringe pump.

The most important parameters effecting nanofiber formation are following: solution properties (polymer molecular weight [18], viscosity [19], surface tension [18, 20] and conductivity [21, 22], process parameters (voltage [18, 22], feeding rate [21, 23], collector type [24–26], distance [22, 27] and ambient parameters (humidity and temperature [28, 29]).

2.2 Experiment. Glass and aluminum foils were used as substrates which collect the fibers. Before deposition the glass substrates were cleaned in ultrasonic bath during 10 minutes. Acetone and methanol were used as solvents for cleaning. After that the substrates were dried in nitrogen gas flow and cleaned in plasma cleaner during 10 min.

Following components were used in process of sol-gel precursor preparation: deionized water, 2-methoxyethanol [C3H8O2] (Sigma-Aldrich, assay ≥ 99.5 %), zinc acetate dihydrate [Zn(CH3CO2)2·2H2O] (Sigma-Aldrich, assay ≥ 99.0 %), aluminium nitrate nonahydrate [Al(NO3)3·9H2O] (Sigma-Aldrich, assay ≥ 98 %), polyvinylpyrrolidone [(C6H9NO)x] (Sigma-Aldrich, Mw 360,000). Amount of these components for the routes #1 and route #2 are pointed in the Table 1.

Table 1. Comparison of preparation procedures for route #1 and route #2.

Material/Procedure	Route #1	Route #2
zinc acetate dehydrate	1 g	1 g
Deionized water	5 ml	2.5 ml
2-methoxyethanol	-	2.5 ml
Aluminium nitrate nonahydrate	1 %	0-3 atomic %
Polyvinylpyrrolidone	0.5 g	0.87 g
Distance between the needle and samples	10 cm	15 cm
Electrospinning voltage	20 kV	14.5 kV
Feeding rate	0.12 μl/min	0.2 μl/min
Drying	-	in air at 150 °C
Annealing	in air, at 100, 300, 400 or 450 °C during 1 hour	in air or in vacuum at 360 °C during 4 hours

Initially zinc acetate dehydrate was dissolved in deionized water or in water mixed with 2-methoxyethanol. Solutions in capped bottles were refluxed by magnetic stirrer at 80 °C during 1 hour. Certain amounts (Table 1) of aluminium nitrate nonahydrate were added as dopant to zinc acetate dehydrate solutions. After 1 hour polyvinylpyrrolidone was added to increase solution viscosity. The solutions were refluxed for 2 hours at the same temperature and transferred into plastic syringes.

The syringe's needle with diameter 0.9 mm was cut in order to have a uniform needle end. The volume of solution intended for the deposition was 1 ml in each case. The fibers were deposited in ambient air. Parameters of electrospinning and subsequent drying and annealing are pointed in the Table 1. Experimental procedure of preparing AZO nanofiber films is represented in flowchart (Fig. 2).

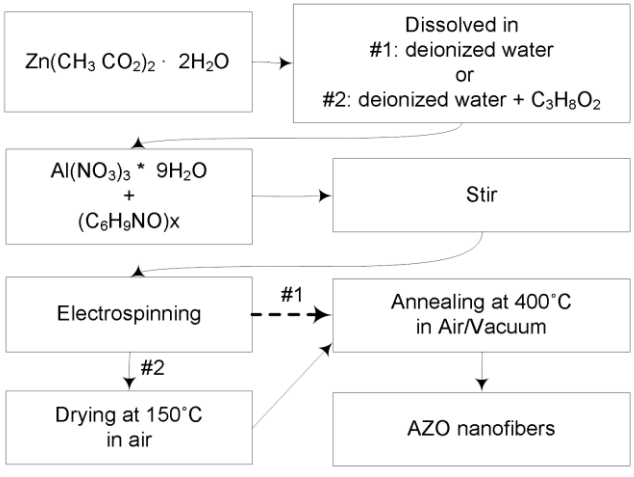

Fig. 2. Preparation of nanofiber films by electrospinning method (routes #1 and #2).

The nanofibers were inspected using on optical microscope (Eclipse E200; Nikon) before annealing. Film transparency was measured by using Spectrophotometer V-570 Jasco. Shape of nanofibers was measured using electron microscopy (HR-SEM; Helios Nanolab, FEI). Element analysis was performed using energy dispersive X-ray spectroscopy (EDS; Oxford Instruments). Nanofiber films were produced on self-assembled electrospinning device with high-voltage power supply (LNC 30000-2pos; Heinzinger) and syringe pump (Multi-Phaser NE-500; New Era).

3. Results and discussions

Mentioned above preparation routes #1 and #2 allows to obtain thin and less thin fibers correspondingly. Route #2 is less sensitive to humidity of the environment. As consequence thick fibers obtained by this route are not suffer from granulation and coalescence.

Optimization of annealing conditions allowed us to overcome the difficulties met by authors [15] and [16] and connected with breaking, granulation and coalescence of thin fibers. Here we describe the logic of this adjustment in more details. Siddheswaran et al. reported in [11] that most of the organic groups are burned at temperature lower than 500 °C. There was no variation in X-ray spectrum of samples annealed at 400 °C, 600 °C and 800 °C [11]. On the basis of this paper one can judge that the variation of annealing temperatures does not change the fiber structure, nevertheless it can change the fiber diameter.

Concentration of elements in atomic % in obtained fibers was measured by energy dispersive x-ray spectroscopy. After annealing total amount Zn, O, and C decreases. Therefore, doped ZnO nanofibers must be thinner after annealing. Indeed in Fig. 3 it is possible to see decreasing diameter of nanofibers with higher temperature and broken fibers at 450 °C. Measured diameters are given in the Table 2. Relative values of O/Zn before and after annealing at 450 °C were 2.1 and 2.9; relative values of C/Zn before and after annealing at 450 °C were 2.6 and 1.48. Consequently, doped ZnO fibers have increased amount of O and decreased amount of C after annealing in air. This regularity is more pronounced at longer annealing times (Table 2).

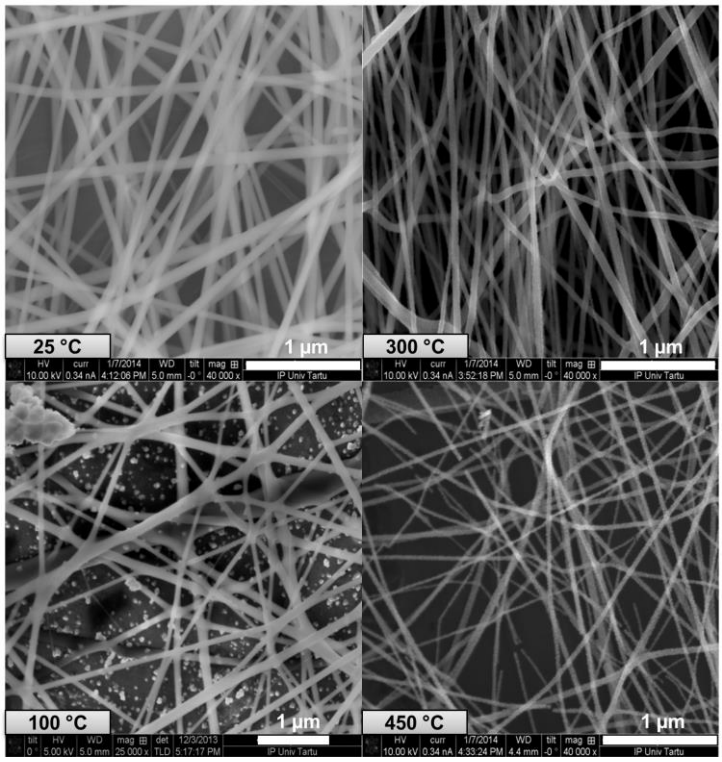

Fig. 3. SEM images of AZO nanofibers annealed at different temperatures. Route #1.

Table 2. Fibers properties: annealing temperature, fiber diameter. Route #1.

Max, annealing temperature °C during 60 min	Average fiber diameter, nm	Annealing procedure time, min	Heating and cooling rate, °C/min
-	95	-	-
100	95	180	1.5
300	57	427	1.5
450	40	627	1.5

It was got 2.4 times shrinkage of fibers after annealing, which is in agreement with the literary data [15]. In a limit, nanofibers can become very thin and can be broken. It can happen because of adhesion and different coefficient of thermal expansion for substrate and as-deposited fibers. To avoid this it is necessary to choose optimal annealing time and temperature.

It was noticed, that broken fibers appeared after annealing at the temperatures between 300 and 450 °C (Fig. 4). Therefore, in route #1 we selected temperature 400 °C, which is intermediate between mentioned ones. To avoid breakage of fibers we used different heating/cooling rates (Table 3). High heating rate led to nanofiber deformation (samples a, b). They lost uniformity and stuck together. Samples c and d with heating rate 4.2 °C/min were cooled fast and slow. They were uniform. Average nanofiber diameter of sample c compare to sample d was bigger because total annealing procedure time was shorter.

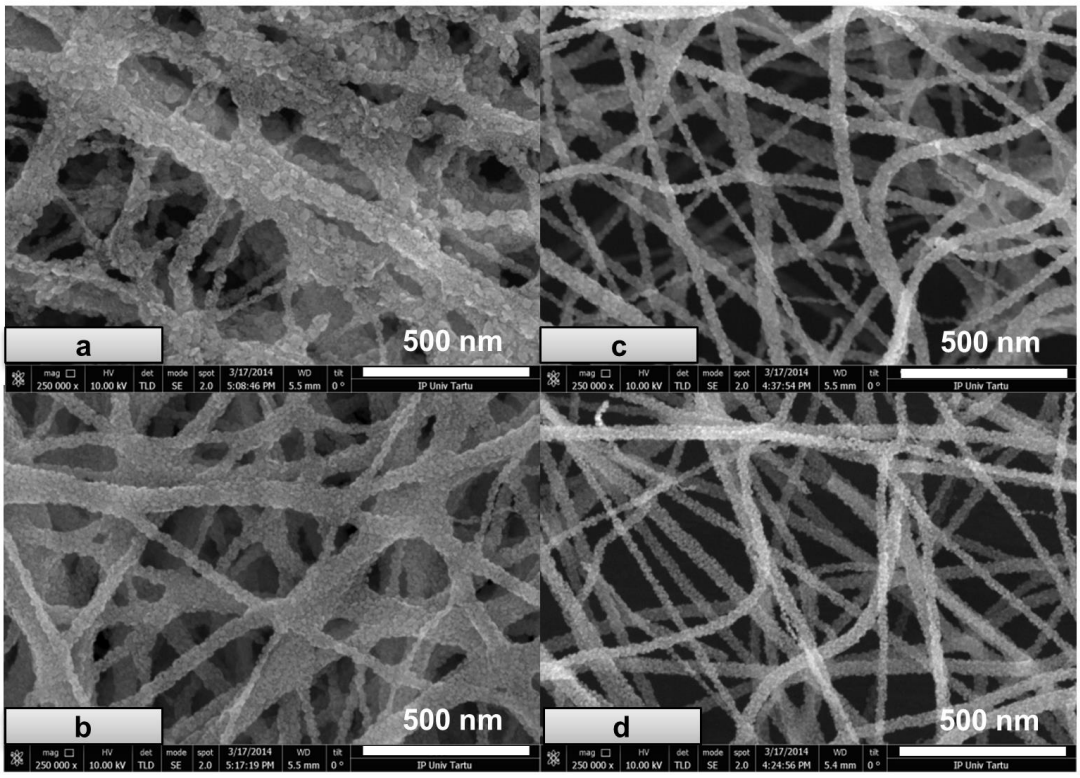

Fig. 4. SEM images of AZO nanofibers annealed with different heating/cooling rate, samples a, b, c and d. Route #1.

Ding et al. got grainlike particles on the fiber surface after annealing [15]. In our case it was possible to affect on grainlike particles size by heating rate. Slow heating rate produce smaller grainlike particles on the fiber surface (Fig. 4a,c). Hence, slow heating rate and longer annealing time are more desirable to produce uniform nanofibers.

In summary, we suggest that annealing at 400 °C with heating rate 4.2 °C/min results in thin fibers with minimal breakage, granulation and coalescence. The influence of cooling rate was not so critical.

Table 3. Fibers properties: heating and cooling rate, fiber diameter. Route #1.

Sample	Max, annealing temperature °C during 60 min	Average fiber diameter, nm	Annealing procedure time, min	Heating rate, °C/min	Cooling rate, °C/min
a	400	84	95	12.5	75.0
b	400	54	120	12.5	12.5
c	400	42	155	4.2	75.0
d	400	31	240	4.2	4.2

Besides annealing temperature and time, it is very important to control of ambient parameters during producing nanofibers. One of these parameters is humidity. Route #1 was implemented at low humidity (15 %). However, solution jet at high humidity (40-70 %) was not enough evaporated during electrospinning process. Fibers could lose their form immediately or later after deposition on substrate and during annealing. Example of producing nanofibers with humidity 66 % from route #1 is shown in Fig. 5.

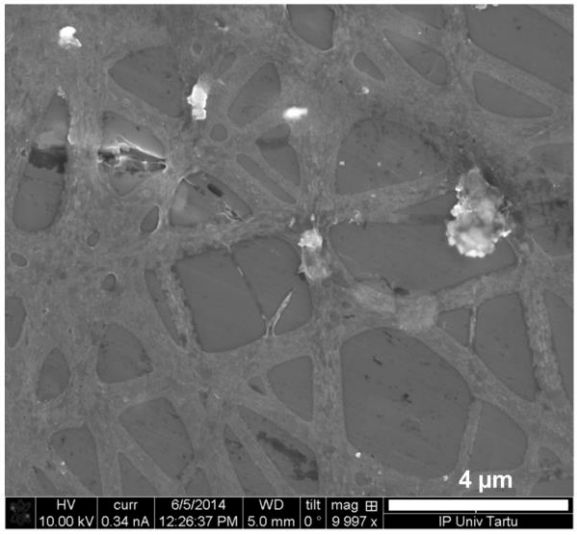

Fig. 5. SEM images of AZO “nanofibers” produced at humidity 66 %. Route #1.

S. Yun at al. [16] got AZO-PVAc nanofibers with different Al doping level. Nanofibers were stuck together and lose their form with increasing Al doping level. They explained it by different ratio of aluminium in solution and did not provide information about humidity level. However, in our case, fibers were uniform with different concentration Al after decreasing influence of humidity (Fig. 6). On this reason we can assume that humidity play more important role than Al content on fiber uniformity.

In order to make solution less sensitive to changes in humidity route #1 was modified. It was necessary to increase solution viscosity and use more evaporated solvent in solution. On this reason, 2-methoxyethanol was added to the solution from route #1. Concentration of polyvinylpyrrolidone was also increased. Additionally, samples were dried before annealing. Modified preparation route was labeled as route #2.

To investigate influence of Al dopant on the zinc-oxide nanofibers formation samples from route #2 were dried at 150 °C in air during 24 hours. Then they were annealed at 360 °C

for 4 hours in air or in vacuum (Fig. 6). Concentration of Al/Zn was varied from 0 to 3 atomic % with step 0.5. Samples with larger Al/Zn ratio had smaller average fiber diameter (Table 4). This behavior can be explained by change in viscosity and conductivity of solution with increasing of Al content [30]. Samples with the same Al/Zn ratio annealed in vacuum or air have approximately the same or slightly larger diameter. However, C/Zn ratio was 4.49 and respectively 0.72. We did not noticed grainlike particles on the fiber surface after annealing in vacuum. We explain this by the burning out of carbon in air atmosphere. Consequently, nanofibers annealed in air have fewer amounts of C, more porous structure and grainlike particles on the fiber surface (Fig. 7).

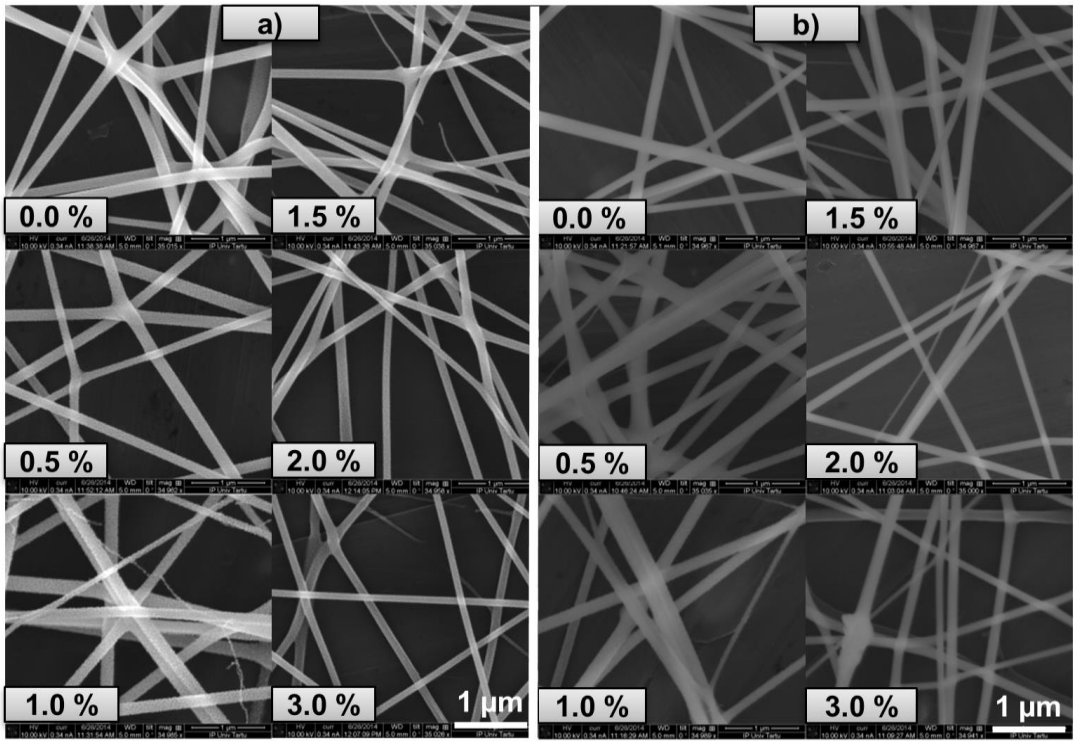

Fig. 6. SEM images of AZO nanofibers prepared by means of route #2 and annealed in: a) air b) vacuum. Concentration of Al/Zn represented in atomic %.

Table 4. Fibers properties: Al/Zn concentration, fiber diameter. Route #2.

Al/Zn, atomic %	Average fiber diameter, nm	
	annealing in air	annealing in vacuum
0.0	140	157
0.5	135	159
1.0	138	157
1.5	130	137
2.0	116	111
3.0	104	108

Nanofibers annealed in air were brighter than those in vacuum according to the SEM images (Fig. 6). It means that individual fibers annealed in air were conductive and they did not charged during SEM measurements. Unfortunately, we did not get as low sheet resistance for AZO nanofiber based films as for spin-coated AZO films [31]. Resistivity measurement procedure assuming to use conductive probes which can damage AZO fibers during the measurements. It can be one of the reasons of measured high sheet resistance.

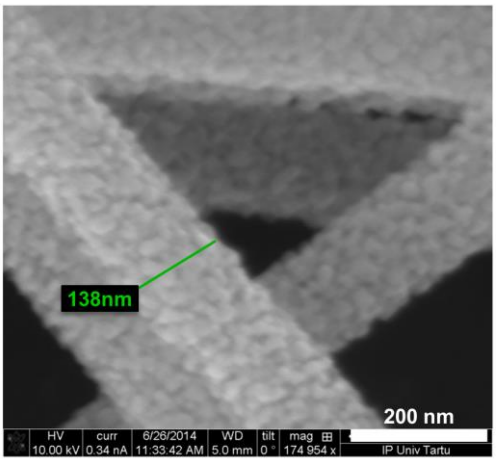

Fig. 7. SEM images AZO nanofibers annealed in air Al/Zn 1 %. Route #2.

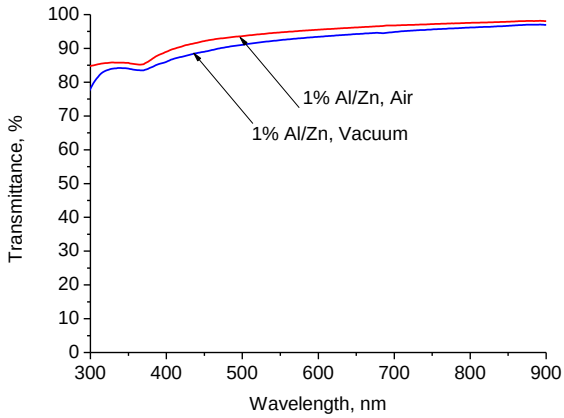

Fig. 8. Transmittance spectra of AZO films annealed in air or vacuum. Route #2.

Fiber networks prepared according to the route #2 and deposited on the glass demonstrated transmittance around 90 % (Fig. 8), which is comparable with ITO [3]. Decreased transmittance of fibers in case of vacuum annealing can be caused by higher amount of residual carbon at such conditions. Firstly, during annealing in air carbon in fibers interacts with oxygen from air and as a consequence huge amount of carbon become burnt out. This statement was proven by element analysis and mentioned above. Secondly, fibers annealed in air and vacuum have approximately the same diameter (Table 4). It means that fibers annealed in air become porous (Fig. 7). On this reason result films can be more transparent.

4. Summary and conclusions

Al doped ZnO films formed from nanofibers were fabricated by electrospinning from sol-gel solution. Parameters of electrospinning, influence of annealing temperatures, annealing speed (heating and cooling), Al dopant concentration and environmental conditions were studied. It was shown that increasing of annealing time or temperature make nanofibers thinner. Longer annealing time lead to a very thin diameter of nanofibers, which can be broken. Slow heating rate and average annealing time are more desirable to produce uniform nanofibers. It was shown that the influence of cooling rate was not so critical.

High and low humidity levels had significant influence on fiber formation and reproducing of results. It was clarified how to prepare samples in both conditions. Al doped ZnO films annealed in air were more transparent than in vacuum. We explained this phenomenon by different ratio of C/Zn, O/Zn in films. Resultant films have potential to be used in optoelectronic devices.

Acknowledgements. *V.I.K. is grateful for the support to European Social Fund's Doctoral Studies and Internationalization Programme DoRa; A.E.R. participation in the analysis of annealing behavior of ZnO fibers was supported through the project № 14-29-00086 of Russian Science Foundation.*

References

[1] http://www.nanocs.com/ITO.htm
[2] T. Minami // *Thin Solid Films* **516** (2008) 5822.
[3] H. Liu, V. Avrutin, N. Izyumskaya, Ü. Özgür, H. Morkoç // *Superlattices and Microstructures* **48** (2010) 458.
[4] C.-Y. Chen, L.-H. Hsiao, J.-I. Chyi // *Journal of Crystal Growth* **425** (2015) 216.
[5] T. Shirahata, T. Kawaharamura, S. Fujita, H. Orita // *Thin Solid Films* **597** (2015) 30.

[6] S. Schubert, F. Schmidt, H. von Wenckstern, M. Grundmann, K. Leo, L. Müller-Meskamp // *Advanced Functional Materials* **25** (2015) 4321.
[7] S. Karakaya, O. Ozbas // *Applied Surface Science* **328** (2015) 177.
[8] Z.-N. Ng, K.-Y. Chan, C.-Y. Low, S.A. Kamaruddin, M.Z. Sahdan // *Ceramics International* **41** (2015) S254.
M. Samadi, H. A. Shivaee, M. Zanetti, A. Pourjavadi, A. Moshfegh // *Journal of Molecular Catalysis A: Chemical* **359** (2012) 42.
[10] S. Yun, S. Lim *// Journal of Solid State Chemistry* **184** (2011) 273.
[11] R. Siddheswaran, R. Sankar, M. Ramesh Babu, M. Rathnakumari, R. Jayavel, P. Murugakoothan, P. Sureshkumar // *Crystal Research and Technology* **41** (2006) 446.
[12] N. Bhardwaj, S. C. Kundu *// Biotechnology Advances* **28** (2010) 325.
[13] M. Kavosh, H. Moallemian, H. Molaei, H. Mehranniya, M. Salami, M.E. Dehdashti *// Synthesis and Reactivity in Inorganic, Metal-Organic, and Nano-Metal Chemistry* **46** (2016) 225.
[14] S. A. Theron, A. L. Yarin, E. Zussman, E. Kroll // *Polymer* **46** (2005) 2889.
[15] B. Ding, T. Ogawa, J. Kim, K. Fujimoto, S. Shiratori // *Thin Solid Films* **516** (2008) 2495.
[16] S. Yun, S. Lim // *Journal of Colloid and Interface Science* **360** (2011) 430.
[17] G. Taylor // *Proceedings of the Royal Society A* **313** (1969) 453.
[18] A.K. Haghi, M. Akbari // *Physica Status Solidi A* **204** (2007) 1830.
[19] J. Deitzel, J. Kleinmeyer, D. Harris, N. Beck Tan // *Polymer* **42** (2001) 261.
[20] M. M. Hohman, M. Shin, G. Rutledge, M. P. Brenner // *Physics of Fluids* **13** (2001) 2221.
[21] W. Zuo, M. Zhu, W. Yang, H. Yu, Y. Chen, Y. Zhang // *Polymer Engineering & Science* **45** (2005) 704.
[22] C. Zhang, X. Yuan, L. Wu, Y. Han, J. Sheng // *European Polymer Journal* **41** (2005) 423.
[23] X. Yuan, Y. Zhang, C. Dong, J. Sheng // *Polymer International* **53** (2004) 1704.
[24] B. Sundaray, V. Subramanian, T.S. Natarajan, R.-Z. Xiang, C.-C. Chang, W.-S. Fann // *Applied Physics Letters* **84** (2004) 1222.
[25] D. Li, Y. Wang, Y. Xia // *Advanced Materials* **16** (2004) 361.
[26] X. Wanga, I.C. Uma, D. Fang, A. Okamoto, B.S. Hsiao, B. Chu // *Polymer* **46** (2005) 4853.
[27] C.S. Ki, D.H. Baek, K.D. Gang, K.H. Lee, I.C. Um, Y.H. Park // *Polymer* **46** (2005) 5094.
[28] C.L. Casper, J.S. Stephens, N.G. Tassi, D.B. Chase, J.F. Rabolt // *Macromolecules* **37** (2004) 573.
[29] C. Mituppatham, M. Nithitanakul, P. Supaphol // *Macromolecular Chemistry and Physics* **205** (2004) 2327.
[30] B. Zhou, Y. Wu, L. Wu, K. Zou, H. Gai // *Physica E: Low-dimensional Systems and Nanostructures* **41** (2009) 705.
[31] V.I. Kondratiev, I. Kink, A.E. Romanov // *Materials Physics and Mechanics* **17** (2013) 38.